EXPERIMENTAL AND NUMERICAL STUDY OF THE CONTINUOUS FLUIDIZED BED DRYER

By

Vladimir Villanueva López

A thesis submitted in partial fulfillment of the requirements for the degree of

MASTER OF SCIENCE

IN

CHEMICAL ENGINEERING

UNIVERSITY OF PUERTO RICO
MAYAGÜEZ CAMPUS
2016

Approved by:

_____	_____
Carlos Velázquez Figueroa, Ph.D President, Graduate Committee	Date
_____	_____
L. Antonio Estévez De Vidts, Ph.D Member, Graduate Committee	Date
_____	_____
Moses N. Bogere, Ph.D Member, Graduate Committee	Date
_____	_____
Paul E. Castillo, Ph.D Representative of Graduate Studies	Date
_____	_____
Aldo Acevedo Rullán, Ph.D Chairperson of the Department	Date

ABSTRACT

Nowadays, batch fluid-bed drying is one of the most efficient drying methods for particulate material; but at the same time, it is the most energy consuming operation in the manufacturing of solid dosage forms. To minimize cost and speed up the production of pharmaceutical products, the continuous manufacturing emerges as an important alternative.

The advantages of this technology in comparison to the batch fluid bed dryer, which is the most predominant in the industry is to reduce cycle times, optimize for faster production, guarantee real-time quality assurance. This work was oriented to understand the continuous fluidized bed drying phenomena by using numerical simulations and experimentation.

I designed a prototype of a continuous fluid bed dryer by using computer aided design CAD coupled with computational fluid dynamic simulations CFD. The equipment promotes back-mixing and the transportation of the particles through the units, by the momentum exerted by the inlet airflow without requiring a mechanical assistant to exit.

The effect of the inlet air velocity and inlet air temperature were evaluated at different initial moisture contents of the lactose granules. A two-phase model proposed by Burgschweiger and Tsotsas[1] included in the processing system engineering tool gSOLIDS for PSE Enterprise was used to understand the interaction of the process parameters with the performance of the novel continuous fluid bed dryer.

The two mass transfer correlations were evaluated to describe the drying kinetics of the particles in the emulsion phase. It was found that the inclusion of the mass transfer correlation proposed by Rhode, result on better predictions of the moisture content of the granules at the outlet of the continuous fluid bed dryer.

Finally, the coupling of computation fluid dynamics with discrete elements methods simulations was used to visualize the fluidization patterns inside the equipment. In this way was possible to visualize the residence time of the particles.

RESUMEN

Actualmente, el secado por lecho fluido por lotes, es una de los métodos más eficientes para el secado de materiales particulados; al mismo tiempo, es una de las operaciones que tienen el mayor consumo de energía en la manufactura de tabletas. Por consiguiente, para minimizar los costos y acelerar la producción de productos farmacéuticos, la manufactura continua se ofrece como una alternativa importante.

La implementación de esta tecnología en comparación con el secado por lecho fluido tradicional, es que reduce el tiempo de operación, se puede alcanzar una mayor producción y se garantiza el control de calidad en tiempo real. Por consiguiente, este proyecto de investigación está orientado a entender el secado continuo por lecho fluido usando simulaciones y experimentación.

Diseñé un prototipo de un secador continuo por lecho fluido fue diseñado usando diseño asistido por computadora acoplado a simulaciones computacionales de fluidos CFD. El equipo proporciona el mezclado de las partículas y el transporte de las mismas a través de la unidad debido al momento impartido por el fluido, de esta manera el equipo no requiere de asistencia mecánica para transportar las partículas hacia la salida del sistema.

El efecto de la velocidad de entrada del aire y la temperatura de bulbo seco, fueron evaluados a diferentes condiciones iniciales de contenido de humedad de los gránulos. El modelo de dos fases propuesto por Burgschweiger and Tsotsas [1] incluido en el programa gSOLIDS por la compañía PSE Enterprise fue usado para entender la interacción de los parámetros de proceso con el rendimiento del prototipo propuesto.

Dos correlaciones de coeficiente de transferencia de masa fueron evaluadas para describir la cinética de secado de las partículas en la fase de emulsión. Se encontró que la inclusión del coeficiente de transferencia propuesto por Rhode, ofrecía mejores predicciones del contenido de humedad de los gránulos a la salida del secador continuo/

Finalmente, fue posible visualizar los patrones de fluidización de los gránulos en el equipo mediante la implementación de simulaciones computacionales de fluidos CFD integradas con simulaciones de elementos discretos DEM y de esta manera fue posible determinar el tiempo de residencia de las partículas.

To God, my parents
Dalgy Lopez, Bladimiro Villanueva
and my sister
Liliana Villanueva
for their love and guidance.
To My uncles, Diego Lopez and Juan Lopez
and My aunt Angela Lopez
for their support.

ACKNOWLEDGEMENT

I would like to express my profound gratitude to God who provides me wisdom, strength and my family for their unconditional love and for being my motivation.

My sincere respect and admiration to my thesis Advisor Dr. Carlos Velazquez for his patience, willingness and support during my studies. I will always remember him for giving me the opportunity to work as a COOP student at Lilly del Caribe and gave me participation in a short project with Bristol-Myer Squibb. Those experiences were significantly important for my professional development and comprehension of the pharmaceutical industry. Also, I want to acknowledge Pedro Hernández y Marcos Rodríguez for their valuable help in the execution of the experiments and simulations.

I would like to thank my graduate committee members: Dr. Antonio L Estévez y al Dr. Moses Bogeres for their comments and suggestions. I want to express my gratitude to Dr. Nelson Cardona and Dr. Carlos Velazquez for allows me to be part of the Pharmaceutical Engineering Education Outreach Program of C-PEDaL because it helps me to improve my teaching skills. I want to thanks the "Pharma Team" Madeline Candelaria, Daniel Mateo, Sonia Avilés, David Mota and Miguel Florian for their companion and encouragement. Also, thanks to Mrs. Carmen Santiago and Mrs. Catherine Pérez for their opportune administrative assistant. Thanks to Pablo López for his assistant in the handling of tool from the workshop to build my prototype.

I also want to acknowledge Angelia Caro from the Graduate Research and Innovation Center (GRIC) of the University of Puerto Rico – Mayaguez Campus Library for her feedback during the writing process.

I wish to acknowledge the University of Puerto Rico at Mayaguez campus and the Engineering Research Center for Structured Organic Particulate Systems (ERC-SOPS, Grant: EEC-0540855) for their financial support.

I want to thanks my friends: Rodinson Arrieta, Martha Rozo, Jorge Perea, Heleine Ramos, Karen Barrios, Ana Reyes, Paul Meza, Christian Luna, Karina Gelis, Gerardo Lopez, Nilsa Paris, Yuan Calderon, Moises de Jesus, Pedro Marín, Brian Montejo, Almodovar Family and all the undergraduates from PESCa.

TABLE OF CONTENT

LIST OF TABLES

LIST OF FIGURES

NOMENCLATURE

X	Moisture content
X_e	Equilibrium moisture content
X_{cr}	Critical moisture content
X_o	Initial moisture content
X_{in}	Inlet moisture content fraction
X_{out}	Outlet moisture content fraction
u_{mf}	Minimum fluidization velocity
u	Inlet velocity
T_{gin}	Temperature of gas inlet
T_{gout}	Temperature of gas outlet
RH_{in}	Relative humidity of gas inlet
RH_{out}	Relative humidity of gas outlet
$K_{Elutriation}$	Elutriation rate
ρ_g	Density of gas
$\rho_{particles}$	Density of particles
g	Gravity
r	Radius particle
$K_{elutriation}$	Rate of elutriation
$\dot{F}_{in}$	Inlet mass flow rate of gas
F_g	Volumetric flow rate of gas
$\dot{F}_{out}$	Outlet mass flow rate of gas
$\dot{M}_{in}$	Inlet mass flow rate of solids
$\dot{M}_{out}$	Outlet mass flow rate of solids
R_{drying}	Overall Drying rate
Sh_{bulk}	Sherwood number bulk of granules
k_c	Mass transfer coefficient
j	Mass flux
Y_{as}	Humidity at adiabatic saturation conditions
Y_{bulk}	Humidity in the gas phase
ν	Normalized drying rate
η	Normalized moisture content
N	Actual drying rate
N_{cr}	Constant drying rate
N_∞	Maximum drying rate deep bed
NTU	Number of Transfer Units
W_G	Mass flow rate of solids
m_s	Mass of solids bed
Sh_{bulk}	Sherwood Emulsion Phase
Sh	Sherwood for a Single particle
Re_0	Reynold
A_p	Surface area of the particles
A_{bed}	Surface area of the
Sc	Schmidt number

CHAPTER 1: INTRODUCTION

1.1 JUSTIFICATION

According to the World Health Organization,“ the global pharmaceutical market was worth US$300 billion in 2014 and is expected to increase 33% within the next three years”[2]. In Puerto Rico, the manufacturing of pharmaceutical products is an important economic activity that generates around 18,000 direct and 68,000 indirect jobs as reported by the Pharmaceutical Industry Association of Puerto Rico (PIA) at their annual meeting in 2012. However, pharmaceutical companies have been forced to downsize due to declining in discovery approval, patent expiration, and marketing of new chemical entities. In orderto sustain profitability the industry can undertake optimization of their manufacturing operations.

The drying process is the most energy consuming operation in the manufacturing of solid dosage forms. Thus, it is important to find economical alternatives to minimize its operational costs. Nowadays, batch fluid-bed drying is one of the most efficient drying methods for particulate material. However, it has been demonstrated that the implementation of the continuous fluid bed dryer is an important alternative. The advantages of this technology in comparison to the batch fluid bed dryer, which is the most predominant in the industry,is to reduce cycle times, optimize for faster production, guarantee real-time quality assurance. Those devices requires smaller facilities which in turn costs less for the company.

Those benefits mentioned cause substantial economic savings, hence the pharmaceutical industry is moving towards continuous manufacturing. Nevertheless, the poor knowledge of the current technology available, the time investment and training due to new regulations and significant changes in operations still pose limitations for some pharmaceutical companies.[3]

This work is focused on the understanding of the continuous fluid bed drying process, that could lead to the development of novel commercial devices. The drying nature of pharmaceutical granules in batch fluid bed drying is the same of the continuous fluid bed drying. However, the residence time is a determinant factor in the overall removal of moisture. The inlet air velocity and the inlet air temperature of the system as well as the initial moisture content of the granules, were factors evaluated during the experimentation.The results obtained were compared with computational simulations to extract valuable insights at different scales (Macroscale -Microscale).

1.2 OBJECTIVES

The purpose of this work was to gain a deeper knowledge of the well-mixed continuous fluid-bed drying process of pharmaceutical granules. That was archived through experimentation along with a comprehensive analysis of computational simulations. The objectives of this research project were to:

- Evaluate the performance of a continuous fluid bed dryer at macro-scale level using a deterministic two-phases model.
- Understand the mechanisms that govern the drying of pharmaceutical granules in a continuous fluid bed.
- Visualize the dynamics of the granules in a novel continuous fluid-bed dryer by the implementation of a two-way coupling simulation of discrete elements methods DEM with computational fluid dynamics CFD.

1.3 LITERATURE REVIEW

1.3.1 Drying Fundamentals

Drying of solids is a process where moisture present in solids is evaporated by an external source of heat and transferred to the surrounding media. Depending on the mechanisms of heat transfer, drying is categorized into convective, contact (conduction), radiant and dielectric or microwave drying. [4]

Around 85% of the industrial dryers are of the convective type[5]. Particularly, fluid-bed dryers have been used successfully for many years to dry a variety of wet particulate materials, such as black tea[6], soybeans [7], yeast[8], bird's chilies[9], among others. The advantage of this technology is the high rates of heat and mass transfer and the low investment and maintenance cost requirement. It also provides a uniform distribution of temperature in the packed bed therefore, for temperature-sensitive materials such as pharmaceutical compounds, food powders and synthetic fertilizer, fluid-bed dryers are the most suitable.

In the fluidized bed drying, a stream of warm dry air flows upward through a bed of wet particles to remove the excess of water on them. For batch fluid-bed drying, a highly uniform distribution of temperature and moisture are obtained therefore, it is considered a well-mixed process.

During the drying of porous granules, the removal of moisture has two stages as shown in **Figure 1** . At the first stage, the drying rate remains constant and the evaporation takes place on the wet surface of the granules. This process continues until the granules reach the critical moisture content. At that point, the surface of the granules is partially dried and the second stage begins.

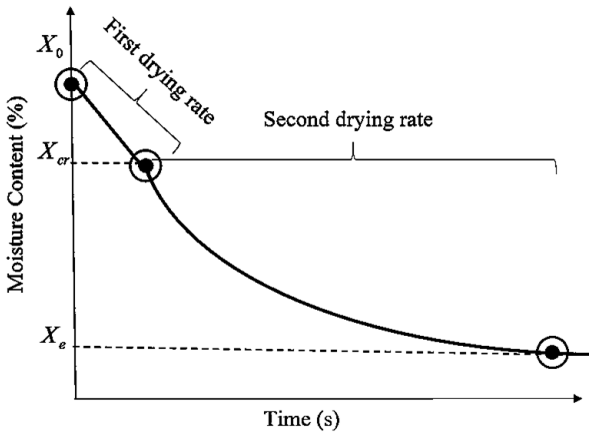

Figure 1. The typical rate of drying curve.

This step is characterized by the diffusion of the remaining moisture from the internal porous of the particles to their surface, where then are evaporated. The drying rate becomes slower and decrease to zero since the system is reaching a thermodynamic equilibrium. The amount of moisture at the end of this stage is called equilibrium moisture content X_e

In order to study fluidized bed drying process in detail, the two-phase mathematical model is roboust alternative [10][11][12]. This model assumes that there is an emulsion phase that includes the particles and the gas in the vicinity and a bubble phase **Figure 2**, which includes a gas phase free of particles. The fraction of gas (v) to each phase is defined by the superficial velocity and the fluidization pattern. As higher the interaction between the phases, the higher will be the heat and mass transfer. The aerodynamics of this model is also extended to the study of catalytic reactors and coal gasification.

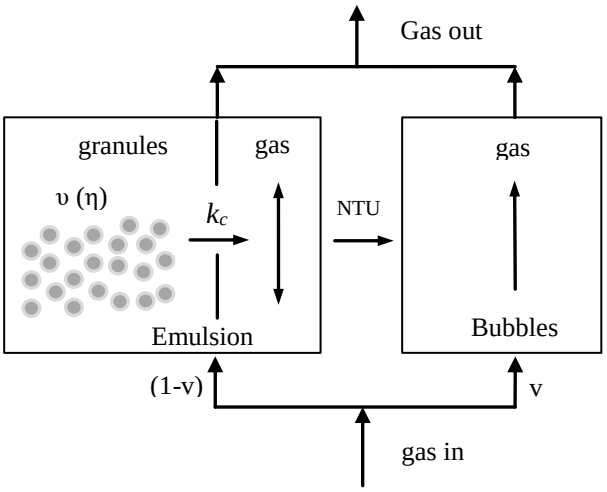

Figure 2. Schematic of a two-phase model.

Within the emulsion phase, the particles transfer moisture to the gas surrounding if defined in term of the normalized drying curve for a single particle υ (η) and the mass transfer coefficient in the emulsion phase k_c.

The normalized drying curve for a single particle is obtained by two different methodologies. The first approach consists in measuring it directly, which is suitable for monodisperse particles [13]. C. Groenewold et al. [14] determined the drying kinetics from a single-particle using an acoustic levitator. That device is also used to determine the drying kinetics of droplets. They characterize γ-Al_2O_3 spheres with an average particle diameter of 1.8 mm. The moisture psortiom isotherm of γ-Al_2O_3 spheres was measured because this information is relevant to determine the equilibrium moisture.

Burgschweiger and Tsotsas [1], highlight that the inclusion of normalized drying curve for a single particle simplify the transformation from batch to continuous. Also, it is possible to perform scale up from the drying from a single particle to a batch system. Or vice versa, obtain the drying kinetics for single particle for solids with particles size distribution by scaling down drying curves obtained from batch fluid bed dryer. In that particular cases is impossible measure directly then additionally to the batch experiments the FLUBED software is required for the scaling down.[15]

On the other hand, mass and heat transfer coefficients within the emulsion phase and additional coefficients for the transfer between phases must be specific. The empirical correlations and the detail equations used in this study will be described in Chapter 3: **Macro – scale simulations – drying performance**

1.3.2 Fluidization

Fluid-bed drying consists of upwards flow gas stream, which passes through a distributor plate, which produces an intimate interaction between the fluid and the particles. As the superficial velocity increases, there is an increase in the pressure drops through porous media, which remains fixed as is shown in **Figure 3**. The air flows through the interstitial space of the particles, which is called porosity (ε). Then, when the drag force exerted by the fluid equals the weight of the particles, they start to fluidize. At that point, the superficial velocity of the fluid is called minimum fluidization velocity (u_{mf}). If the superficial velocity increases further, the pressure drop remains constant, and the fluidization takes place.

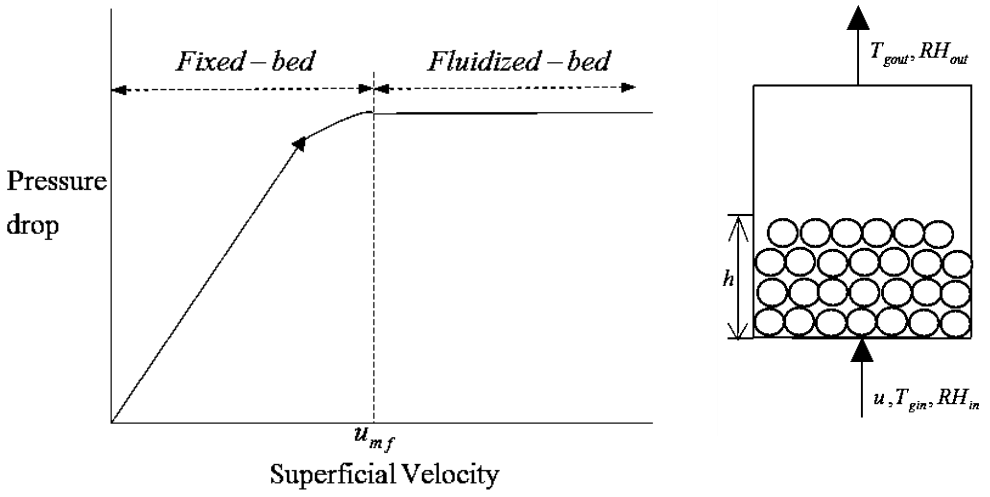

Figure 3. Pressure drop in a packed bed with the increment of the superficial velocity.

Several empirical correlations to compute the minimum fluidization velocity have been published [16]. *Geldart* [17] proposed a classification of the particles depending on the characteristics of the fluidization displayed **Table 1**.

Table 1. Geldart classification [17]

Classification	Description
Group A (30-150 μm) and (<1.4 g/cm^3)	Aeratable particles, dense phase expansion after minimum fluidization, before bubbling starts.
Group B (40-500 μm) (1.4 - 4 g/cm^3)	Sand-like particles, start bubbling at minimum fluidization
Group C (d < 30 μm)	Fine and ultra-fine particles, difficult to fluidize due to the cohesive forces
Group D (d > 500 μm)	Large and dense particles, poor fluidization due to the formation of large bubbles in the bed.

The characteristics of the particulate material are determinant, as well as the mass flow rate of the fluid, in the fluidization pattern. Depending on the purpose, the fluid volumetric flow requirements change and it might then be possible that the applicability of an existent device is limited for all type of materials.

For instance, a material with particle size smaller than 30 μm, classified as Geldart Group C, display strong cohesive forces. This behavior significantly impair the ability to fluidize them. In contrast, for Group D, the gravitational forces are higher. Therefore, the required velocity to fluidize them is greater than the required by Group C.

The drying process affects the fluidization pattern significantly due to the removal of moisture, which makes particles lighter. For that reason, drier particles will have a different Geldart group classification and become easier to fluidize.

The fluidization pattern affects the mass and energy transfer significantly. Many empirical correlations have been widely reported in the literature to estimate both transfer rate. In this project, two specific empirical correlations were evaluated and are described in detail in Chapter 3.

1.3.3 Continuous fluid-bed drying

Continuous manufacturing has demonstrated significant advantages in comparison with the batch processes; for instance, the amount of product that can be processed. Another advantage is the impact of real-time monitoring in the quality of the drug products since one

can have way higher percentage of scrutiny in the continuous approach. In addition, the implementation of that technology represents a significant reduction of energy consumption as well as optimization of industrial facilities space due to those equipment requiring smaller facilities [18].

An industrial well-mixed continuous fluid-bed dryer is shown in **Figure 4**. The wet material is continuously fed into the unit forming a packed bed of particles. Two sections can be identified: the first section is called the drying section where the removal of moisture takes place. The amount of material retained is determined by the weir height, which is located at the end of each section. In the second section, cool air is fed to cool down the particles, which will be transferred to the next stage of the process.

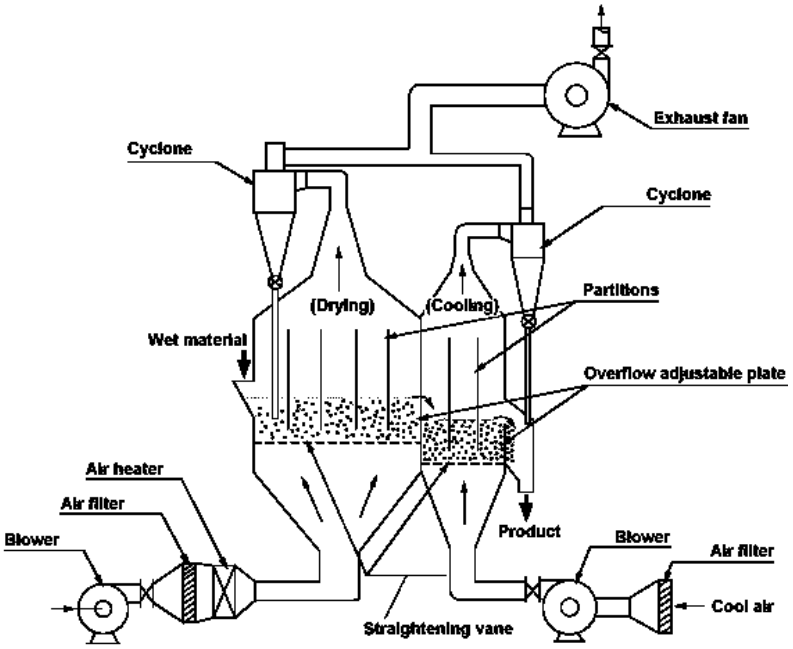

Figure 4. Horizontal Multiple-chamber Continuous Fluid Bed Drying and Cooling System. Digital image. Continuous Fluid Bed Drying System. Kurimoto Ltd, n.d. Web. 25 Aug. 2016. <http://www.kurimoto.co.jp/worldwide/en/product/item/07pw/330.php>.

According to Mujumdar [5], there are two types of continuous fluid bed dryers depending on the movement of the particles inside the equipment, well-mixed fluid-bed dryer and plug flow fluid-bed dryer. In the first one, the vessel usually has a length to a wide ratio less than 5:1. Particle mixing is in both directions, horizontal and vertical, producing a disperse phase with the highly uniform distribution of temperature.

On the other hand, the plug flow fluid-bed dryer vessel usually has a length to the wide ratio in the range of 5:1 to 30:1. The vertical mixing is higher than the horizontal one. Some of these devices include an agitator to promote the back mixing of solids and their movement

through the unit. A wide distribution of residence time of the particles in this system results in a diverse moisture content at the outlet of the system.

Continuous fluid bed drying is a complex process to study due to the coupled simultaneous mass and heat transfer. Also, particulate systems behave in a completely different way than liquid and gas. In addition, the hydrodynamics and the material properties of the solids change during the operation and therefore the drying rate is affected. The study of the continuous fluid bed dying process may be addressed depending on the level of detail or complexity, which it could be related to the purpose of the model. For instance, some models could be used for design, performance evaluation for deep analysis of the phenomenon.

Depending on the level of complexity they are categorized into three main groups. The first group corresponds to lumped models; by coupling the drying curves obtained from a batch fluid bed dryer with some equations that describe the residence time of the particles may enable the determination of the moisture of the particles at the outlet [19][20]. McKenzie and R. E. Bahu [21], proposed the following equation to approximate the average moisture content at the outlet of a well-mixed fluid bed dryer.

$$X_0 = \frac{1}{\tau_b}\int_0^{\infty} X(t)\exp\left(-\frac{t}{\tau_b}\right)dt \qquad (1.1)$$

X (t) represents the evolution of the moisture content in a bed of particles being dried at a constant temperature. τ_b accounts for the mean residence time of the particles in the bed. The main limitation of these types of models is their applicability for scaling up. However, due to their simplicity, they can be used as a first approximation.

The second group is the deterministic models; they describe the mass and heat transfer between particles and the air. From that approach, it is possible to obtain relevant information about the process because the equations do have physical meaning. Researchers have proposed a variety of deterministic models at different spatial scale depending on the level of detail to be studied [22].

Mathematical models at macro scale (~ 10^{-2} – 10^{1} m) and meso scale (~ 10^{-4} – 10^{-2} m) are the most common used, and the reason is that the drying process is dominated by large-scale parameters in most cases. For instance, some researchers have found that the drying rate is affected by the height of the bed significantly[23][24]. Thus, it is impractical to use a sophisticated model that requires the estimations of difficult-to-measure parameters at the micro-scale level. For example, it is impractical to use the latter approach if one wishes to determine the drying time in an existing device.

Macro-scale modeling is preferred since its scale is relevant for the industry and allows the researcher to perform a quick analysis of this process. Hence, they are useful for industrial design and optimization. Finally, the macro scale requires less consumption of computational resources because fewer distributed parameters must be calculated in comparison with micro-scale models [1].

Burgschweiger and Tsotsas [1] proposed a two-phase model to study the continuous fluid-bed drying process and validated it at steady-state and dynamic conditions. The experiments were carried out using the particles characterized by C. Groenewold et al. The model assumes a well-mixed fluid bed dryer, and a populations balance approach was included to predict the moisture content of the particles according to their residence time.

Alaathar et al. [25], developed a flowsheet simulation of a continuous fluid bed dryer within the software called SolidSim using a two-phase model based on the previous works of Burgschweiger and Tsotsas [1]. They also extended the applicability of the model considering the particles size and moisture distribution. However, no experiments were carried out to validate the simulations.

For this research project, a lab-scale prototype of a continuous fluid bed dryer was proposed and constructed. The effect of the superficial velocity and the temperature of inlet air on the performance of this device was studied. A comprehensive analysis was carried out by the implementation of a two-phase model included in advanced process modeling software gSOLIDs. However, a different approach was used to define the drying kinetics of the emulsion phase. The drying kinetics from a single-particle was avoided and instead, it was based on the drying kinetics from a bulk of lactose granules with an average size of 1500 μm. It was assumed that during the drying process the falling rate was only present. However, it was assumed that the porosity of the granules did not present a significant resistance to the drying process.

1.4 Overview of research work

The analysis of the continuous fluid bed dryer is described in this document as follow: Chapter 1 previous works have been related to the continuous fluid bed drying process, drying mechanism and objectives of this project. Chapter 2 includes the experimental study; the inlet velocity and the temperature of the air were evaluated as well as the initial moisture content of the granules to determine their effect on the drying efficiency. In Chapter 3, computational simulations at macro-scale level were used and provided insights about the process. The

experimental results were contrasted to the simulations. Two different mass transfer empirical correlations were evaluated to predict the final moisture content.

Chapter 4 includes some computational simulations at micro-scale level. Computational fluid dynamics simulations were used as initial step in the design of the continuous fluid bed dryer. After several trial and errors, the optimal design was constructed and validated experimentally. Additionally, Computational Fluid Dynamics and Discrete Elements Methods were integrated to predict the flow of the granules inside the system. This was helpful to identify dead spots at the dryer and to have a better understanding of fluidization pattern in this equipment. Finally, Chapter 5: Conclusions and recommendation includes overall conclusions and recommendation for future work.

CHAPTER 2: EXPERIMENTAL STUDY OF CONTINUOUS FLUID-BED DRYER

2.1 EQUIPMENT DESCRIPTION

To carry out the experiments, the conical vessel of the batch fluid bed dryer, Aeromatic STREA-1™ shown in **Figure 5**, was replaced by new vessel appropriate for continuous fluid bed drying. The new vessel was obtained after testing several CAD designs on Multiphysics software, called Star-CCM+, which is a powerful tool to perform computational fluid dynamics simulations. The objective was to design a vessel that provides proper distribution of the air across the freeboard to promote the movement of the particles through the unit while they become dried. More details about the development and the computational simulations involved in the design of this vessel are reported in Chapter 4.

The equipment consists of a blower that provides a volumetric flow from 40 to 120 m^3/h. The unit had a resistance temperature device (RTD) sensor near the entrance of the vessel to measure the inlet air temperature and sends that signal to a control system, a DeltaV System by Emerson™. The control system adjusts the electrical current of an electric heating coil to provide the amount of heat require to reach the desired temperature of inlet air. The operating temperature of the inlet air flow is controlled in the range between 50 to 100 °C.

Figure 5. Batch fluid bed dryer (FBD) Aeromatic STREA-1™.

A schematic of the continuous fluid bed dryer is shown in **Figure 6**. The lab-scale vessel was constructed with of poly (methyl methacrylate) Plexiglas®; The channel is 0.12236 m long, 0.04968 m wide and the weir is 0.0143 m height.

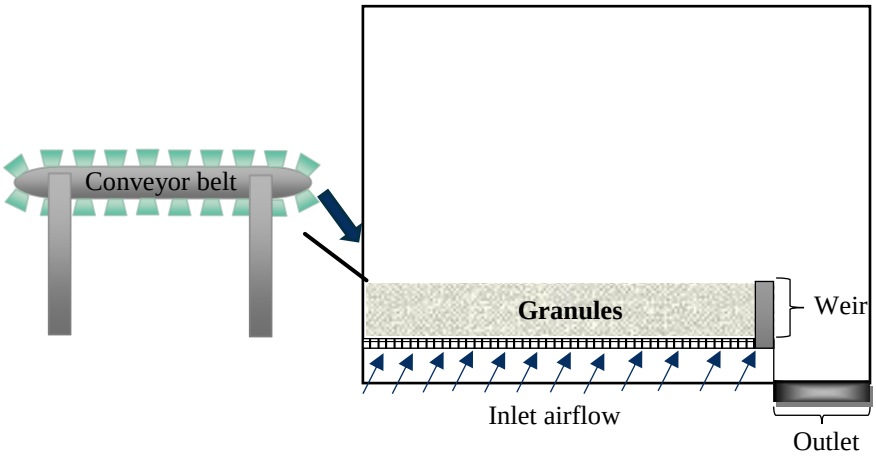

Figure 6. Schematic drawing of the continuous fluid bed dryer.

Wet granules were fed by a conveyor belt with adjustable speed. Several cups were attached to the surface of the conveyor, and each one was filled with 3 g of wet lactose granules. The speed of the conveyor belt was set-up to obtain a mass flow rate of 3 g/s. Once the granules were fed into the vessel, they interacted with a stream of warm air promoting the movement of them through the chamber and to finally flow over the weir. Some samples of granules were collected at the outlet to determine moisture content. A schematic of the continuous fluid bed dryer is shown in **Figure 6**, and further details of the interaction of the gas with the granules is reported in Chapter 4.

2.2 MATERIALS AND METHOD

2.2.1 Materials description

A blend of mono-hydrated and anhydrous lactose granules was sieved using two sieve mesh number 14 and mesh 10 on the Tyler scale. Only the particles retained on the sieve 14 were used in this study. The average size of the particles was to 1595 mm and bulk density 489.2 kg/m^3

2.2.1.1 Moisture sorption isotherm

From the moisture sorption isotherm, it is possible to estimate the equilibrium moisture content of the granules. In **Figure 7**, is the dynamics sorptiom shown for anhydrous lactose, DuraLac® , which does not contain water of crystallization according to the supplier[1]. As we

[1] Meggler (Excipients and Technology)

observe the amount of water that can retain is lower at highly humidity environments. The sorption isotherm is required for the two-phases model included in gSOLIDS, found in Chapter 3, because this provided the equilibrium moisture content in powders in relation with the relative humidity of the surrounding environment.

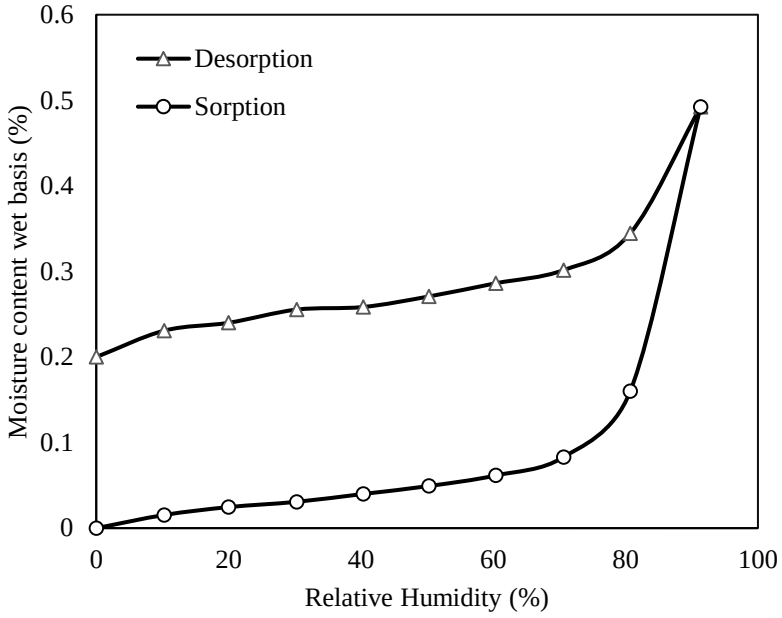

Figure 7. Dynamics vapor psortion at 20°C for Anhydrous lactose, DuraLac® H.

2.2.2 Methodology

Experimental designs were proposed to determine the effect of the superficial velocity and temperature at a different initial moisture content of the solids over the drying time of the granules and shown in **Figure 8**. The black dots represent the experiments carried out, while the white dots represent those that were no possible to conduct due to technical difficulties. However, it was possible to obtain relevant information about the process.

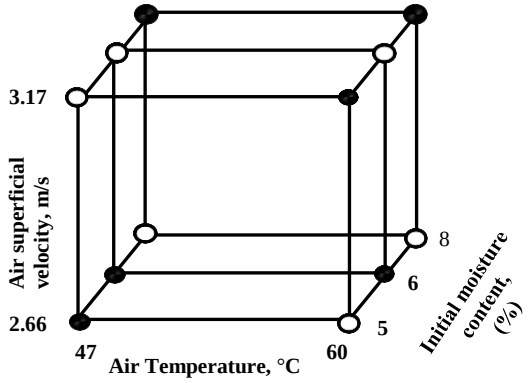

Figure 8. The design of experiments DoE.

2.2.2.1 Wet material preparation

The granules were sieved and then wetted gravimetrically using a peristaltic pump to archive the desired moisture content. Then the moisture content of the solids was measured by using a Loss on Drying analyzer. The analysis consists of heating 5 g sample for 15 minutes at 70 °C, after that, the change in weight of the sample is associated with the moisture evaporation.

2.2.2.2 Moisture content analysis

2.2.2.3 Sampling

Five samples were collected every five seconds after solids start to flow over the weir. Then the sampling time was extended to ten seconds to obtain a total of fifteen samples. Each sample was weighted, and their moisture content was measured using a loss on drying analyzer.

2.2.3 Results and Discussions

Table 2. summarize the results of the experimental design. That percentage of removal of moisture has proportional relations with superficial velocity and temperature of the dry air inlet. However, the velocity inlet of the air affect significantly the residence time of the particles, that means that even when a high superficial velocity leads to a higher mass transfer coefficient, it also affects the hydrodynamics. Particles that do not have enough residence time will not be dried enough when they leave the system earlier. The amount of heat supply to the particles determine the rate of removal of moisture; therefore, the best combination of the operational parameters corresponds to approximately 59°C and 2.68 m/s of the velocity inlet leading to a 64.93 % of the initial moisture.

Table 2. Experimental results

Experimental Run	Average Initial moisture (%)	Initial Moisture (%)	Air Inlet Temperature (°C)	Superficial velocity (m/s)	Average moisture content outlet (%)	Percent removal (%)
1	5.08	4.93	46.3	2.19	3.11	36.9
2		5.16	48.1	2.66	3.00	42
3		5.14	59.5	3.16	2.12	58.9
4	6.66	6.47	47.0	2.66	3.33	48.6
5		6.86	58.7	2.68	2.41	64.9
6	8.21	7.97	47.9	3.14	4.43	44.5
7		8.45	59.7	3.17	5.66	33.0

As we can see in **Table 2**, the experimental run #4 (47.0 ˚C, 2.66 m/s) presented a high variability of the mass flow rate at the outlet of the systems. That could be associated with accumulation of the particles; however, it was expected to obtain a high variability of the moisture content of the particles at the outlet. However, that was not the case.

As we can see in **Figure 10**, on last experiment the inlet air conditions were 3.17 m/s and 59.7 ˚C; and the granules had the higher initial average moisture content as well, of 8.21% wet basis. At those conditions, the particles were heavier to be fluidized and the residence time was enough to remove the moisture content partially.

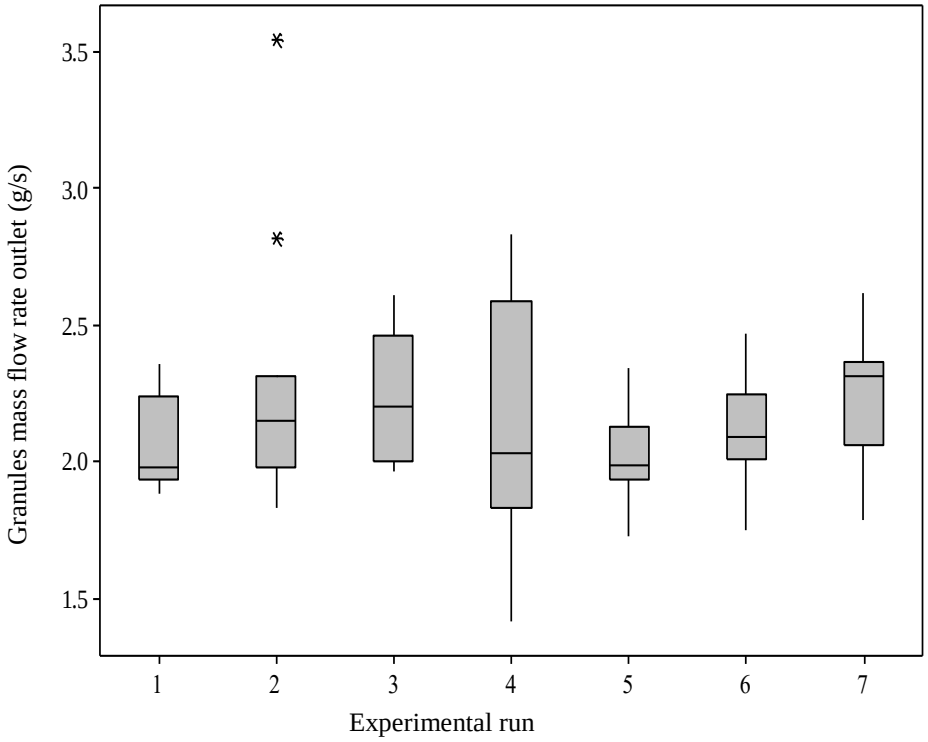

Figure 9. Boxplot of granules mass flow rate at the outlet of the CFBD.

The inlet superficial velocity is an important parameter since it is directly related to the convective mass transfer and affects the residence time of the particles. The velocity of the inlet must be higher enough to remove moisture as much as possible but not too high to provide the granules enough residence time to get dried. On the other hand, as the temperature of the inlet air increase so does the percentage of removal, but it must be not too high because the pharmaceutical powders are sensitive to temperature and could be damaged.

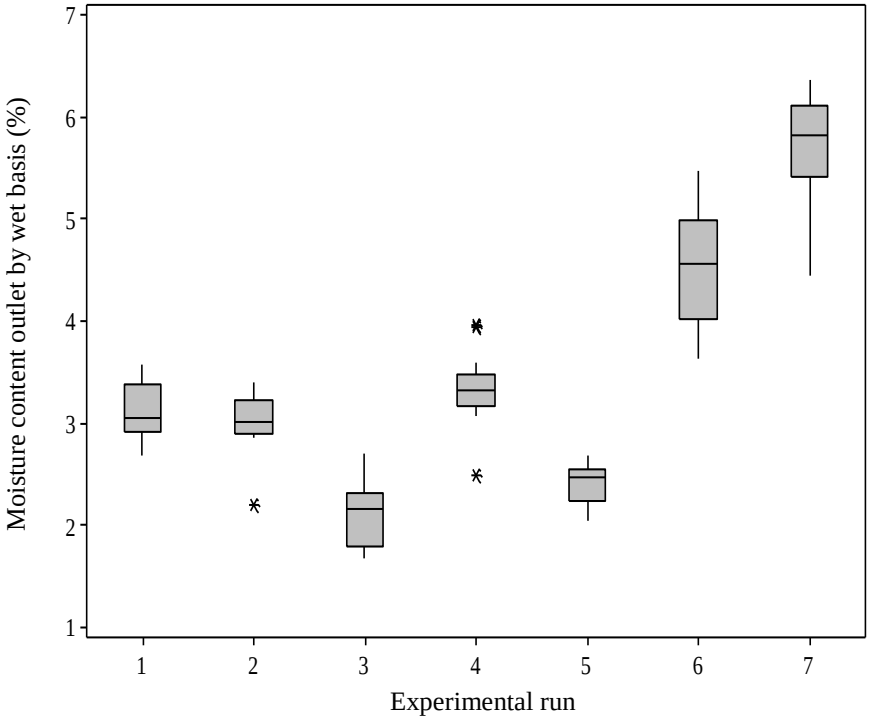

Figure 10. Boxplot of moisture content in wet basis for each experimental run.

Flowsheet simulation is a process system engineering tool, useful to simulate industrial processes. It is also helpful in the design process and optimization. The unit operations in this platform are entities that contain the mathematical models and correlations that describe their behavior. Unit operations such as powder blending, size reduction, sizing, granulation, drying, and tablet compression as entities can be connected to simulate a production line. Multiple scenarios can be evaluated by sensitivity analysis changing operational parameters. A screenshot of a flowsheet simulation of a continuous fluid bed dryer in gSOLIDS is shown in **Figure 11**.

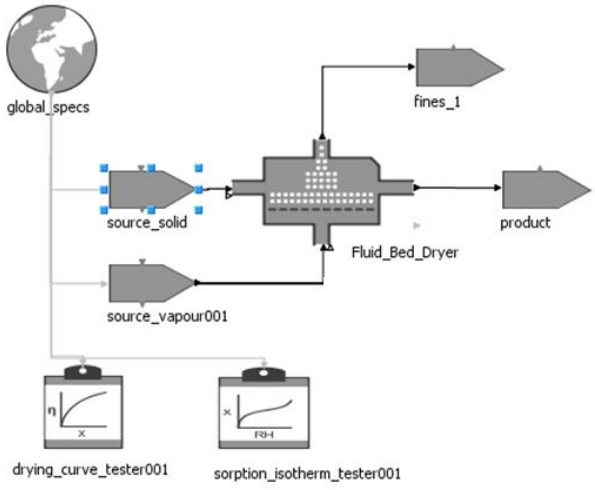

Figure 11. Flowsheet simulation of a continuous fluid bed dryer on gSOLIDS.

The performance of accurate predictions of the whole process requires the validation of each unit operation within this simulation environment. That is achieved by estimating the relevant parameters of the mathematical model that describe their behavior in experiments carried out on the real equipment.

Once the model is validated, it is possible to obtain insights of the process that would not be possible to observe by simple experimentation and could be used to improve the control system capability. Also, it is possible to evaluate multiple scenarios within the design space without requiring additional experiments. As a result, that would represent a reduction in time and cost. In the next sections, a description of the components of the mathematical model of the continuous fluid bed dryer used for this study and found in the software gSOLIDS is described in details.

3.1 HYDRODYNAMICS EFFECT

The wet granules were fed to the dryer at a constant mass flow rate. The model assumes that the Elutriation take place immediately as the granules entered the system. the equations reported by Zenz and Weil describe the amount of material elutriated base on the density of the particles and the superficial velocity of the air.

$$\frac{K_{Elutriation}}{\rho_g u} = 1.26x10^7 \left(\frac{u^2}{rg\rho_{particles}^2} \right)^{1.88} \quad only\ for \left(\frac{u^2}{rg\rho_{particles}^2} \right) < 3x10^{-4} \tag{3.1}$$

$$\frac{K_{Elutriation}}{\rho_g u} = 4.51x10^7 \left(\frac{u^2}{rg\rho_{particles}^2} \right)^{1.88} \quad only\ for \left(\frac{u^2}{rg\rho_{particles}^2} \right) > 3x10^{-4} \tag{3.2}$$

$K_{elutriation,}$ represents the rate of material elutriated. Since the experiments were run at low superficial velocity, the height of the packed bed of granules did not expand significantly forming a holdup of material and avoiding a large elutriation. The granules moved through the vessel in full contact with the air causing a well-mixed state until they flowed over the weir.

3.2 MASS AND ENERGY BALANCES

The set of differential equations that describe the mass and energy balance are complemented by some empirical correlations of mass transfer. The aggregation, breakage or shrinkage of the granules was no present during the experiments. The heat losses were assumed negligible.

Mass balance of moisture - vapor phase

$$\frac{dM_{vap}}{dt} = \dot{F}_{in} Y_{in} - \dot{F}_{out} Y_{out} + R_{drying} \tag{3.3}$$

Mass balance of moisture - solid phase

$$\frac{dM}{dt} = \dot{M}_{in} X_{in} - \dot{M}_{out} X_{out} - R_{drying} \tag{3.4}$$

Energy balance

$$\frac{dH_p}{dt} = \dot{M}_{in}\, h_{in} - \dot{M}_{out}\, h_{out} - \Delta H_{drying} \tag{3.5}$$

$$H_p = M_{total,p} h_p \tag{3.6}$$

$$h_p = f\left(T_p, P, x_p\right) \tag{3.7}$$

3.2.1 Drying rate

In this mathematical model, it is assumed that the falling drying rate dominates the drying kinetic of the particles. That means that the diffusion of the moisture from the surface to the environment limited the transfer of moisture. The overall drying rate is defined by the following expression.

$$R_{drying} = A_p\, j \tag{3.8}$$

$$j = \nu \rho_g k_c \left(Y_{as} - Y_{bulk}\right) \tag{3.9}$$

A_p represents the superficial area of the granules, j is the mass flux and depend on the mass transfer coefficient k_c ,the gradient of humidity in the gas phase Y_{bulk} and the humidity at adiabatic saturation conditions Y_{as} and the normalized drying rate for a single particle ν .

3.2.1.1 Normalized drying curve

The method was proposed by Van Meel [26], and consists of the compilation of multiples drying curves into a single characteristic normalized drying curve for the material of interest. The normalization is defined as the normalization of the drying rate as a function of the normalized moisture content (3.10).

$$\nu = \left(\eta\right) \tag{3.10}$$

The normalization of the drying rate ν (Eq. 3.11) is obtained dividing the actual drying rate by the first drying rate (constant).

$$\nu = \frac{N}{N_{cr}} \tag{3.11}$$

On the other hand, the normalized moisture content is defined by the following expressions

$$\eta = \frac{\left(X - X_e\right)}{\left(X_{cr} - X_e\right)} \tag{3.12}$$

$$X_e = f\left(\mathrm{RH}_{\mathrm{in}}\right) \tag{3.13}$$

Here, X represents the moisture content at any instant, X_e**,** the equilibrium moisture content and X_{cr} the critical moisture content respectively. The equilibrium moisture is the amount of water that the solids can retain in equilibrium with the humidity of the environment (3.13). Therefore, the psortion isotherm curve of the lactose granules provides information to estimate it.

3.2.1.2 Universal Drying Curve UDC

In this project, due to the limitations to measuring the normalized drying curve for a single particle for the granules, the universal drying curve UDC with adjusted NTU (number of transfer units) was chosen as an alternative to providing that important information. The definition of universal drying curve was reported in previous works by Kemps [27] and shown in equations (3.12). Measuring the humidity of the air once it pass through the bulk of granules. This simple approach has been used in deep bed of granules good predictions.

$$N = N_{cr}\left(\frac{1 - e^{-\eta\, NTU}}{1 - e^{-NTU}}\right) \tag{3.14}$$

In the expression above, N represents the actual drying rate of the granules and N_{cr} represents the maximum theoretical drying rate or in other words the constant drying rate.

Notice that η is equal to 1 during the constant rate and in the falling drying rate period is estimated by the equation (3.12).

$$N_{cr} = N_{\infty}\left(1 - e^{-NTU}\right) \tag{3.15}$$

In the expression above, N_{∞} represents the maximum drying rate, and this approximation is obtained by considering a volumetric rate of air passing through an infinitely deep bed of granules.

$$N_{\infty} = \left(\frac{W_G\left(Y_{as} - Y_{in}\right)}{m_s}\right) \tag{3.16}$$

The Number of Transfer Units (NTU) is related to the proximity of outlet air to the saturation due to the moisture exchange with the granules. Therefore, the N_{cr} depend on the height of the packed bed.

The NTU was an adjustable parameter, and it was found that five Number of Transfer Unit was the appropriated value since the height of the bed was small. Higher values of NTU require deeper bed of granules.

3.2.1.3 Mass transfer correlations

Once the normalized drying rate for the granules is define (ν). The next step is to calculate the mass transfer coefficient k_c from equation (3.16)

$$\mathrm{Sh}_{\mathrm{bulk}} = \frac{k_c d_p}{D} \tag{3.17}$$

From the equation above D, correspond to the diffusivity of the liquid from the surface to the environment. d_{p}, correspond to the particles size.

3.2.1.3.1 Burgschweiger and Tsotsas [1]

In correlation (3.17), $\mathrm{Sh}_{\mathrm{bulk}}$ is denominated the apparent Sherwood number transfer, which includes the effect of back-mixing and it is estimated from the real Sherwood number obtained from the single particle (3.18).

$$\mathrm{Sh}_{\mathrm{bulk}} = \frac{\mathrm{Re}_0 \mathrm{Sc}}{\frac{A_p}{A_{bed}}} \ln\left(1 + \frac{\mathrm{Sh}\frac{A_p}{A_{bed}}}{\mathrm{Re}_0 \mathrm{Sc}}\right) \tag{3.18}$$

$$\mathrm{Sh} = 2 + 0.6\,\mathrm{Re}_0^{\left(\frac{1}{2}\right)} \mathrm{Sc}^{\left(\frac{1}{3}\right)} \tag{3.19}$$

$$\mathrm{Sc} = \frac{\mu_g}{\rho_g D_i} \tag{3.20}$$

$$\mathrm{Re}_0 = \frac{d_p u_0 \rho_g}{\mu_g} \tag{3.21}$$

$$u_0 = \frac{F_g}{\rho_g A_{bed}} \tag{3.22}$$

3.2.1.3.2 Rhode [28]

The correlation proposed by Rhode (3.22), only depend on the Reynold number

$$Sh_{bulk} = 0.03\,\mathrm{Re}_0^{1.3} \tag{3.23}$$

3.3 RESULTS AND DISCUSSION

The experimental conditions for the experimental run were reported in Chapter 2: Experimental study of continuous fluid-bed dryer and below there are samples of the simulations. The dots correspond to the experimental data.

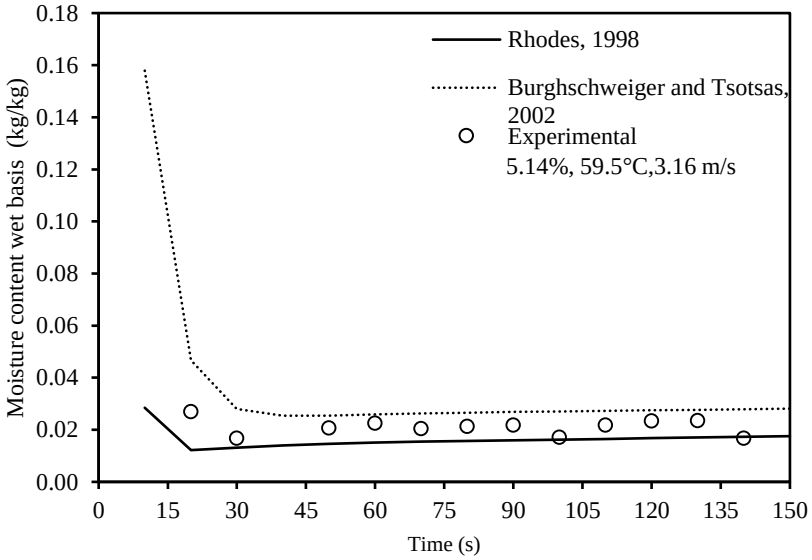

Figure 12. Moisture content vs time for experimental run 3

The elutriation of particles during the execution of the experiments was negligible. Thus, the granules move through the device while becoming dried and then flow over the weir to the outlet of the continuous fluid bed dryer. The results obtained from the simulations overestimated the outlet mass flow rate of the granules because it does not account for how the air distribution over the freeboard affects the movement of the particles. Therefore, the residence time of the granules does not match with the results of the computational simulations

On the other hand, it was found that the predictions of the granule moisture content at the outlet of the continuous fluid bed dryer with the empirical correlation of the mass transfer proposed by Burgschweiger and Tsotsas were higher in comparison with the experimental results. It could be associated with a mixed effect of a low residence time of the granules and

the nature of the drying regime accounted by the model. Thus, the two-phase model used in this study only considers the falling drying rate regime, and it is possible the granules also display the constant drying rate regime not accounted for by the model. That means that, even though the dimensions of the device were small, the granules could evaporate the water bounded to the surface faster than the predicted by the simulations using the Burgschweiger and Tsotsas correlations for the mass transfer.

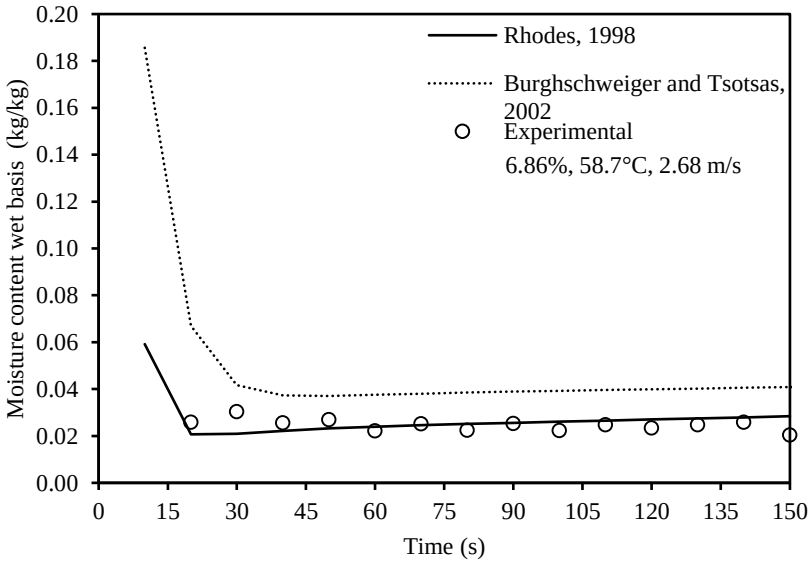

Figure 13. Moisture content vs time for experimental run 5.

In contrast, the predictions of the moisture content of the granules at the outlet using the mass transfer correlation proposed by Rhode estimated significantly well for the superficial velocity of 2.66 m/s. It is worth mentioning that, the mass transfer correlation proposed by Rhode (3.20) is simpler in comparison with the correlations proposed by Burgschweiger and Tsotsas, and their approximation were more close to the experimental results.

The implementation of both correlations is useful to predict the lower and upper limits of the granules moisture content.

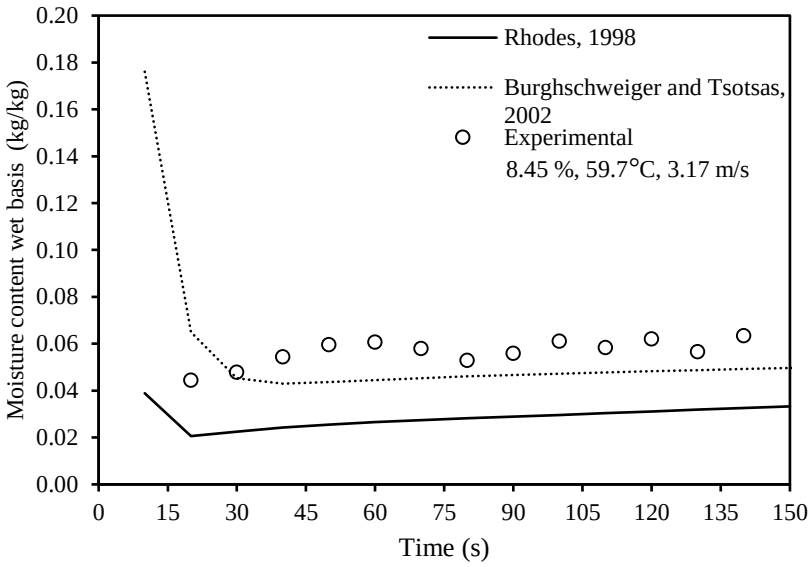

Figure 14. Moisture content vs time for experimental run 7

CHAPTER 4: MICRO- SCALE SIMULATIONS - HYDRODYNAMICS ANALYSIS

The simulations included in this chapter were performed with two objectives:

1. Design an appropriate vessel of a continuous fluid bed dryer to promote the movement of the particles from the entrance to the outlet of the system. That was archived using computational fluid dynamics simulations to evaluate multiples design of the continuous fluid bed dryer.
2. To obtain a visualization of the distribution of granules in the final design by coupling Computational Fluid Dynamics simulations with Discrete Element Methods.

4.1 COMPUTATIONAL FLUID DYNAMICS SIMULATIONS

Computational fluid dynamics is a discipline within fluid mechanics useful to predict the fluid flow through a geometry of interest. The simulations comprise solving the momentum, mass and energy balance by using computational algorithms. The steps of the whole process are summarized in **Figure 15**.

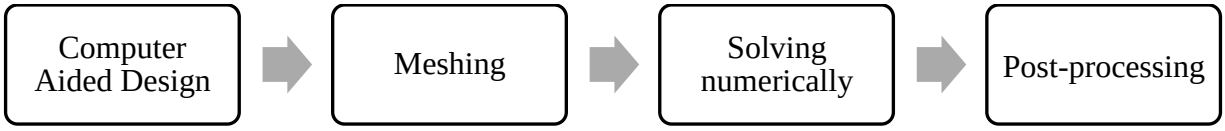

Figure 15. Flowchart of the Computational Fluid Dynamics

4.1.1 Computer Aided Design

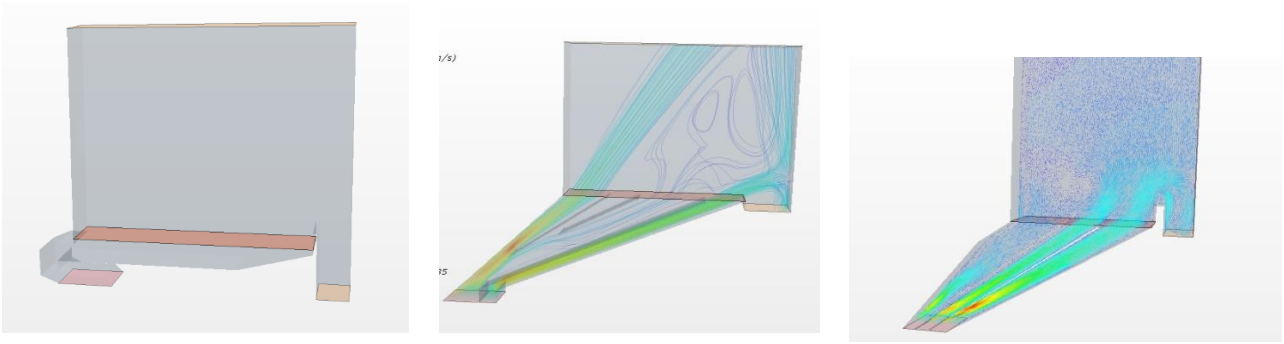

Figure 16. Some of the previous computer aided designs tested on Star-CCM+

During this stage, several designs were created and evaluated in Star-CCM+ to visualize how the air distribute over the freeboard to promoted the movement of the particles from the entrance to the outlet. After several trials and error, the design shown in **Figure 17** displayed a

better distribution of the air across the freeboard in comparison with the previous designs shown **Figure 16**.

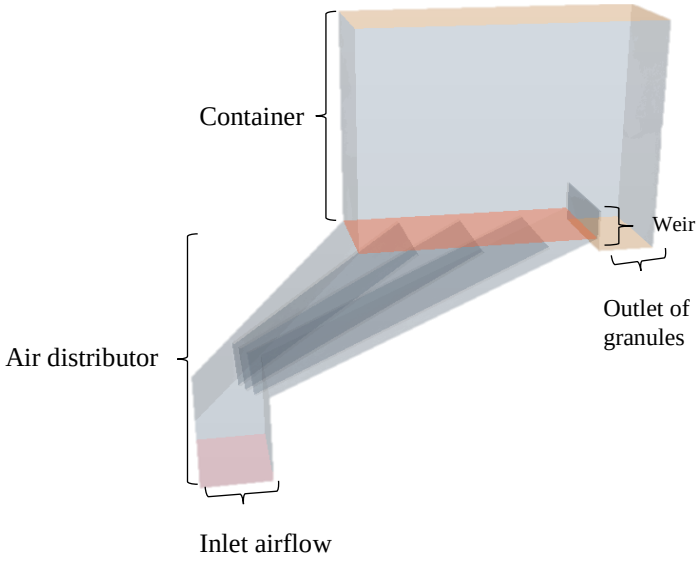

Figure 17. The prototype of the continuous fluid bed dryer.

It is worth mentioning that this vessel was built with sheets of Methyl Methacrylate and the experiments were reported in Chapter 2. The vessel is divided into two main sections: the first section is air distributor, the which has three sheets that promote the distribution of the air across the freeboard. The second section is the container, which holds the granules forming a bed defined by the height of the weir.

4.1.2 Meshing process

This process consists in the discretization of the domain defined by the geometry of interest into some small volumes or subdomains. Each volume is called cell. The accuracy of the solutions obtained depends on the quality of the meshing and the size of the cells.

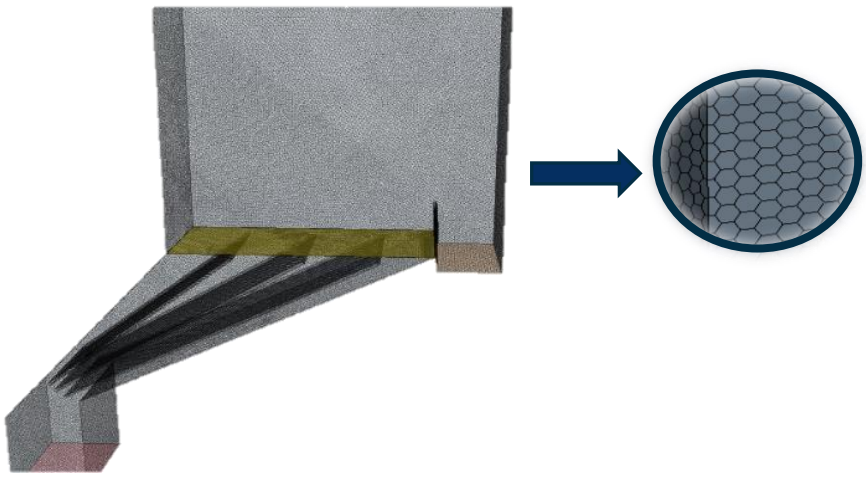

Figure 18. Meshing of the prototype

The computation power required to perform the computations is higher as the number of cells increase. The 3D CAD of the continuous fluid bed dryer was meshed in polyhedral cells with of 0.001 m size to obtain a total of 645.395 cells **Figure 18**.

4.1.3 Solving numerically

The Two-Layer K-epsilon turbulent model was used to describe the fluid flow through a geometry of interest. The term K refers to the component of kinetic turbulent, while epsilon represents the turbulent dissipation. This model was selected because it is simple in comparison with the existent turbulent models and it is flexible regarding meshing. It can be used for high-Reynolds number and provide good results at low-Reynolds numbers where the viscous forces are dominant, and it is required fine meshes to capture the details close to the boundary layer. It has also demonstrated reasonable results even in the coarse mesh. The documentation provided by the Star-CCM+ recommended this turbulence model as a default if there is no certainty about the type of turbulent model to choose.

Table 3. Computational Fluid Dynamics Parameters

Flow type	Turbulent
Gas phase	Eulerian
Wall boundary conditions	No Slip
Time step used	0.001s
Convergence criteria	10^{-3}
Maximum solid packing volume fraction	0.63
Mesh	Hexagonal
Outlet pressure	Atmospheric

4.2 DISCRETE ELEMENTS METHODS

Discrete elements method is a numerical method developed by Cundall and Strack [29] to predict the flow of granular material. The algorithm calculates resulting forces and the new position of the particles each time step because of the collision of them. In most of the cases, these simulations assume that the particles are spheres.

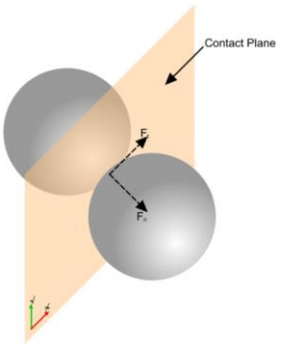

Figure 19. Discrete Elements Methods. Image was taken from Star-CCM+ manual

For this study, the system of granules was modeled over the soft-sphere method. This consideration accounts the deformation of the particles. Some of the forces estimates in the coalitions include Normal forces such as Normal spring force and damping force. Moreover, tangential forces such as tangential spring forces and tangential damping forces. Also, Rolling friction forces.

4.3 COUPLING COMPUTATIONAL FLUID DYNAMICS AND DISCRETE ELEMENTS METHODS

To obtain a visualization of the distribution of the particles inside the unit, a coupled simulations of discrete elements method and computational fluid dynamics was performed. Coupling CFD-DEM required intense calculations and the level of details desire to obtain will depend on the computation power available. The simulation mode used was two-way coupling, where each module exchanges information in both directions to perform the calculations.[30]

In these simulations, the fluid flow is described by the Navier-Stoke equations with the continuity equations. The CFD solver estimates the velocity profile as well as all the properties related to the fluid. After that, that information is integrated with the relative velocity of the particles loaded in the geometry of interest. From the interaction between the surrounding fluid and the particles is possible to estimate the drag force.

Once the drag force exerted by the fluid on the particles is calculated, that information is transferred to the Discrete Elements Methods solver to update the new position of the particles. The porosity of the medium change, due to the relocation of the particles. As a new fluid field is estimated based on the porosity of the medium.

.

To capture the interaction of the fluid with the DEM particles, the size of the mesh in the container increased to five times the size of the particles. The objective was to visualize the distribution of particles in the bed and their residence time. The simulation parameters are compiled in the Appendix of this document.

4.4 RESULTS AND DISCUSSION

The behavior of the particles inside the continuous fluid bed dryer is depicted in **Figure** . For easier visualization, the DEM results and CFD results displayed separately, however, the coupling of both were present during the simulation time. The picture in the upper row, shown the behavior of the particles when they are in contact with the fluid. The color of the particles represents their residence time in labels.

During the first seconds, the particles move across the bed and start to accumulate close to the weir in the chamber **Figure** .**a1.** Notice that almost after 20 seconds the particles accumulated forming a packed **Figure 22.a3**. On the other hand, **Figure** .**b1, b2, b3** are the results of CFD. The colored horizontal bar represents the distribution of velocities across the board**.** There is a reduction of the velocity close to the walls and close to the sheets. The velocity of the fluid close to the weir is higher in comparison with the other section of the board to flow over the weir the particles accumulated in that section. The residence time for a distribution of particles could be visualized and what is necessary to provide sufficient residence time so that the desired water removal is achieved.

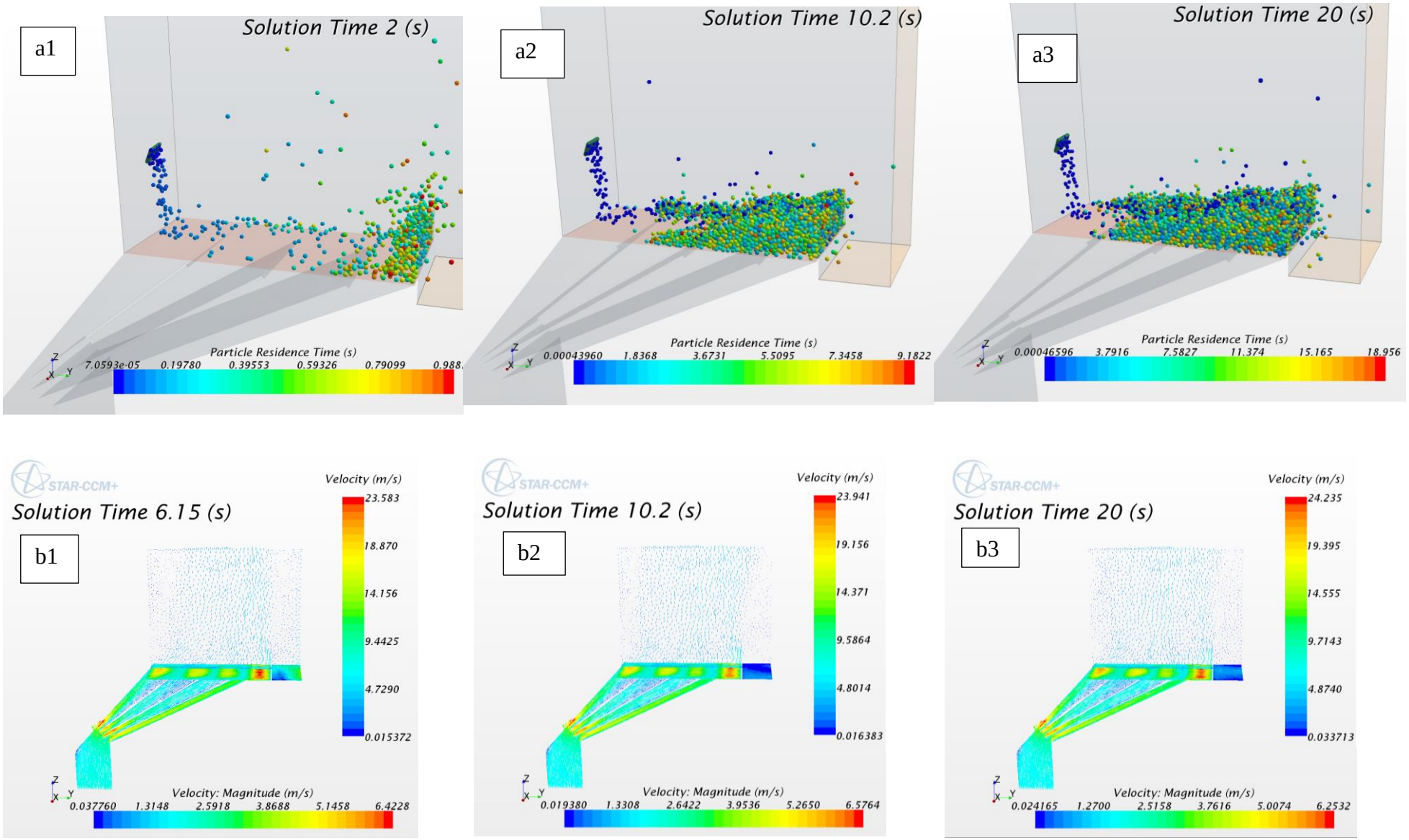

Figure 20. CFD-DEM Simulation inlet air velocity 6.65 m/s

CHAPTER 5: CONCLUSIONS AND RECOMMENDATIONS

A two-phase model proposed by Burgschweiger and Tsotsas include in the process engineering tool gSOLIDS from the company PSE Enterprise was used to study the continuous fluidized bed drying process of pharmaceutical granules. A simplified version of the model was implemented. The experimental results were compared with the results obtained from the simulations. It was found that the two-phase model makes better predicts of the moisture content at the outlet of the system with the mass transfer correlation proposed by Rhode which depends only on the Reynold number. The results obtained from experimental and simulations models concur that at optimal parameters, 69.26% removal of moisture can be expected.

The temperature of the inlet air was the most significant parameter in operation for the removal of moisture. On the other hand, the air inlet velocity is an important parameter since it is directly related to the convective mass transfer and affects the residence time of the particles. The velocity of the inlet must be higher enough to remove moisture as much as possible but not too high to provide the granules enough residence time to get dried.

The universal drying curve UDC is a practical strategy to obtain the drying kinetics from a batch fluidized bed dryer. To design a continuous fluidized bed dryer, applied the extension of the universal drying curve and integrate that with the two-phase model is a relevant strategy.

The coupling simulations DEM-CFD were appropriate to visualize the fluidization pattern and identify dead spots inside the system. It was observed a back mixing of the particle inside the chamber, which corresponds with the assumptions of the two-phases model. On the other hand, the design of the chamber was possible by the design aided with computational fluid dynamics.

REFERENCES

[1] J. Burgschweiger and E. Tsotsas, “Experimental investigation and modelling of continuous fluidized bed drying under steady-state and dynamic conditions,” *Chem. Eng. Sci.*, vol. 57, no. 24, pp. 5021–5038, Dec. 2002.

[2] “Pharmaceutical Industry.” [Online]. Available: http://www.who.int/trade/glossary/story073/en/.

[3] K. Plumb, “Continuous Processing in the Pharmaceutical Industry,” *Chem. Eng. Res. Des.*, vol. 83, no. 6, pp. 730–738, Jun. 2005.

[4] A. Mujumdar, “Principles, Classification, and Selection of Dryers,” in *Handbook of Industrial Drying, Third Edition*, CRC Press, 2006.

[5] C. L. Law and A. S. Mujumdar, “Fluidized Bed Dryers,” in *Handbook of Industrial Drying, Third Edition*, CRC Press, 2006.

[6] S. J. Temple and a. J. B. van Boxtel, “Modelling of Fluidized-bed Drying of Black Tea,” *J. Agric. Eng. Res.*, vol. 74, no. 2, pp. 203–212, Oct. 1999.

[7] G. R. Luz, W. A. dos Santos Conceição, L. M. de Matos Jorge, P. R. Paraíso, and C. M. G. Andrade, “Dynamic modeling and control of soybean meal drying in a direct rotary dryer,” *Food Bioprod. Process.*, vol. 88, no. 2–3, pp. 90–98, Jun. 2010.

[8] H. Akbari, K. Karimi, M. Lundin, and M. J. Taherzadeh, “Optimization of baker’s yeast drying in industrial continuous fluidized bed dryer,” *Food Bioprod. Process.*, vol. 90, no. 1, pp. 52–57, Jan. 2012.

[9] S. M. Tasirin, S. K. Kamarudin, K. Jaafar, and K. F. Lee, “The drying kinetics of bird’s chillies in a fluidized bed dryer,” *J. Food Eng.*, vol. 79, no. 2, pp. 695–705, Mar. 2007.

[10] B. Paláncz, “A mathematical model for continuous fluidized bed drying,” *Chem. Eng. Sci.*, vol. 38, no. 7, pp. 1045–1059, 1983.

[11] C. Srinivasakannan and N. Balasubramanian, “An Analysis on Modeling of Fluidized Bed Drying of Granular Material,” *Adv. Powder Technol.*, vol. 19, no. 1, pp. 73–82, Jan. 2008.

[12] M. R. Assari, H. Basirat Tabrizi, and M. Saffar-Avval, “Numerical simulation of fluid bed drying based on two-fluid model and experimental validation,” *Appl. Therm. Eng.*, vol. 27, no. 2–3, pp. 422–429, Feb. 2007.

[13] M. Peglow, T. Metzger, G. Lee, H. Schiffter, R. Hampel, S. Heinrich, and E. Tsotsas, “Measurement of Average Moisture Content and Drying Kinetics for Single Particles, Droplets and Dryers,” in *Modern Drying Technology*, vol. 2, Weinheim, Germany: Wiley-VCH Verlag GmbH & Co. KGaA, 2011, pp. 1–71.

[14] C. Groenewold, C. Möser, H. Groenewold, and E. Tsotsas, “Determination of single-particle drying kinetics in an acoustic levitator,” in *Chemical Engineering Journal*, 2002, vol. 86, pp. 217–222.

[15] T. K. B. Fajar and A. M. Praba, “Derivation of Single Particle Drying Kinetics of Tapioca Flour,” vol. 5, no. 5, pp. 565–570, 2013.

[16] R. Coltters and A. L. Rivas, “Minimum fluidation velocity correlations in particulate systems,” *Powder Technol.*, vol. 147, no. 1–3, pp. 34–48, Oct. 2004.

[17] D. Geldart, “Types of gas fluidization,” *Powder Technol.*, vol. 7, no. 5, pp. 285–292, May 1973.

[18] S. T. F. C. Mortier, T. De Beer, K. V Gernaey, J. P. Remon, C. Vervaet, and I. Nopens, “Mechanistic modelling of fluidized bed drying processes of wet porous granules: a review.,” *Eur. J. Pharm. Biopharm.*, vol. 79, no. 2, pp. 205–25, Oct. 2011.

[19] M. Khanali, S. Rafiee, A. Jafari, and A. Banisharif, “Study of Residence Time Distribution of Rough Rice in a Plug Flow Fluid Bed Dryer,” *Int. J. Adv. Sci. Technol.*, vol. 48, pp. 103–114, 2012.

[20] P. Bachmann and E. Tsotsas, “Analysis of Residence Time Distribution Data in Horizontal Fluidized Beds,” *Procedia Eng.*, vol. 102, pp. 790–798, 2015.

[21] K. A. McKenzie and R. E. Bahu, “Material model for fluidised bed drying,” *Drying*, vol. 91, pp. 130–141, 1991.

[22] T. Defraeye, “Advanced computational modelling for drying processes – A review,” *Appl. Energy*, vol. 131, pp. 323–344, Oct. 2014.

[23] L. Garnavi, N. Kasiri, and S. H. Hashemabadi, “Mathematical modeling of a continuous fluidized bed dryer,” *Int. Commun. Heat Mass Transf.*, vol. 33, no. 5, pp. 666–675, May 2006.

[24] R. Prommas, “Theoretical and experimental study of heat and mass transfer mechanism during convective drying of multi-layered porous packed bed ☆,” *Int. Commun. Heat Mass Transf.*, vol. 38, no. 7, pp. 900–905, 2011.

[25] I. Alaathar, E.-U. Hartge, S. Heinrich, and J. Werther, “Modeling and flowsheet simulation of continuous fluidized bed dryers,” *Powder Technol.*, Apr. 2012.

[26] D. A. van Meel, “Adiabatic convection batch drying with recirculation of air,” *Chem. Eng. Sci.*, vol. 9, no. 1, pp. 36–44, Aug. 1958.

[27] I. C. Kemp, “Drying models, myths, and misconceptions,” *Chem. Eng. Technol.*, vol. 34, no. 7, pp. 1057–1066, 2011.

[28] M. Rhodes, *Introduction to Particle Technology*. Chichester, UK: John Wiley & Sons, Ltd, 2008.

[29] P. A. Cundall and O. D. L. Strack, “A discrete numerical model for granular assemblies,” *Géotechnique*, vol. 29, no. 1, pp. 47–65, Mar. 1979.

[30] M. Liu, Y. Wen, R. Liu, B. Liu, and Y. Shao, “Investigation of fluidization behavior of high density particle in spouted bed using CFD-DEM coupling method,” *Powder Technol.*, vol. 280, pp. 72–82, 2015.

APPENDIX A: MOISTURE CONTENT VS TIME

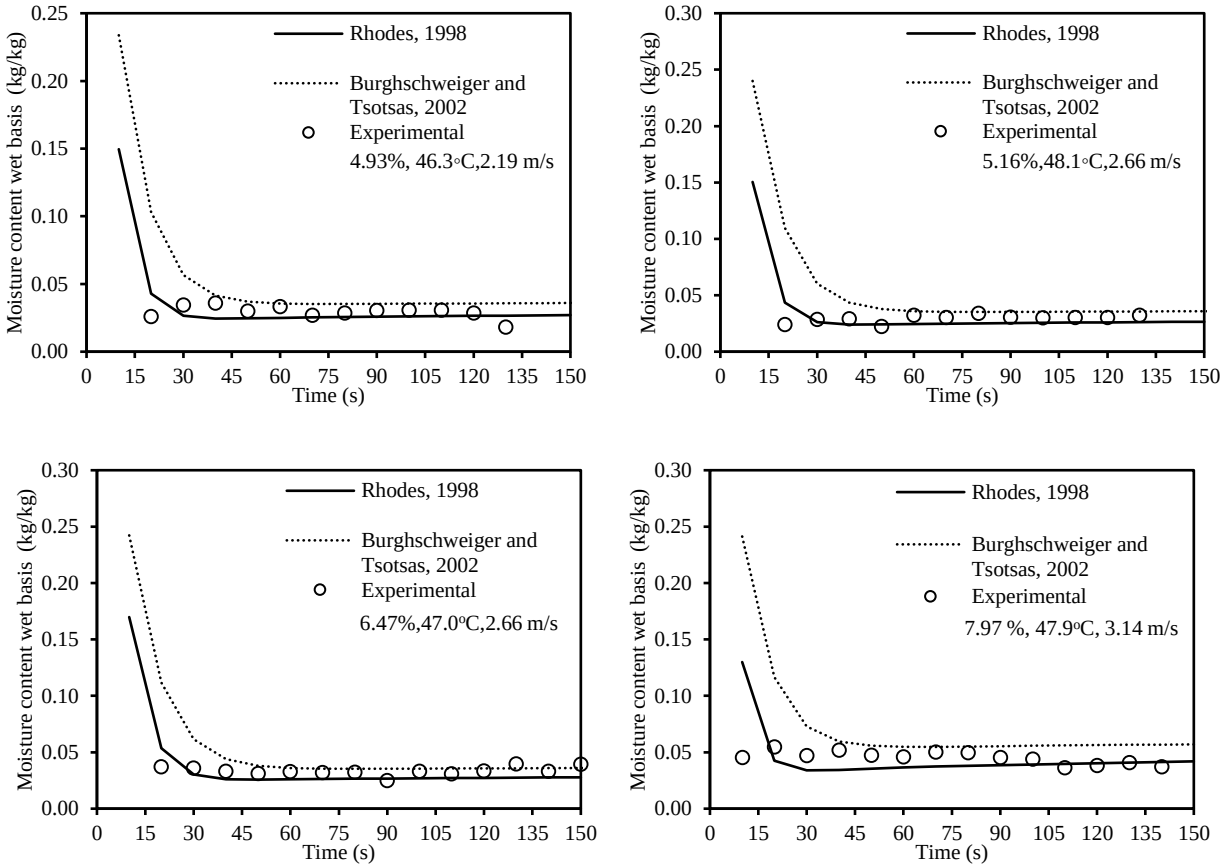

Figure A. 1 Results of moisture content vs time comparison with numerical simulations.

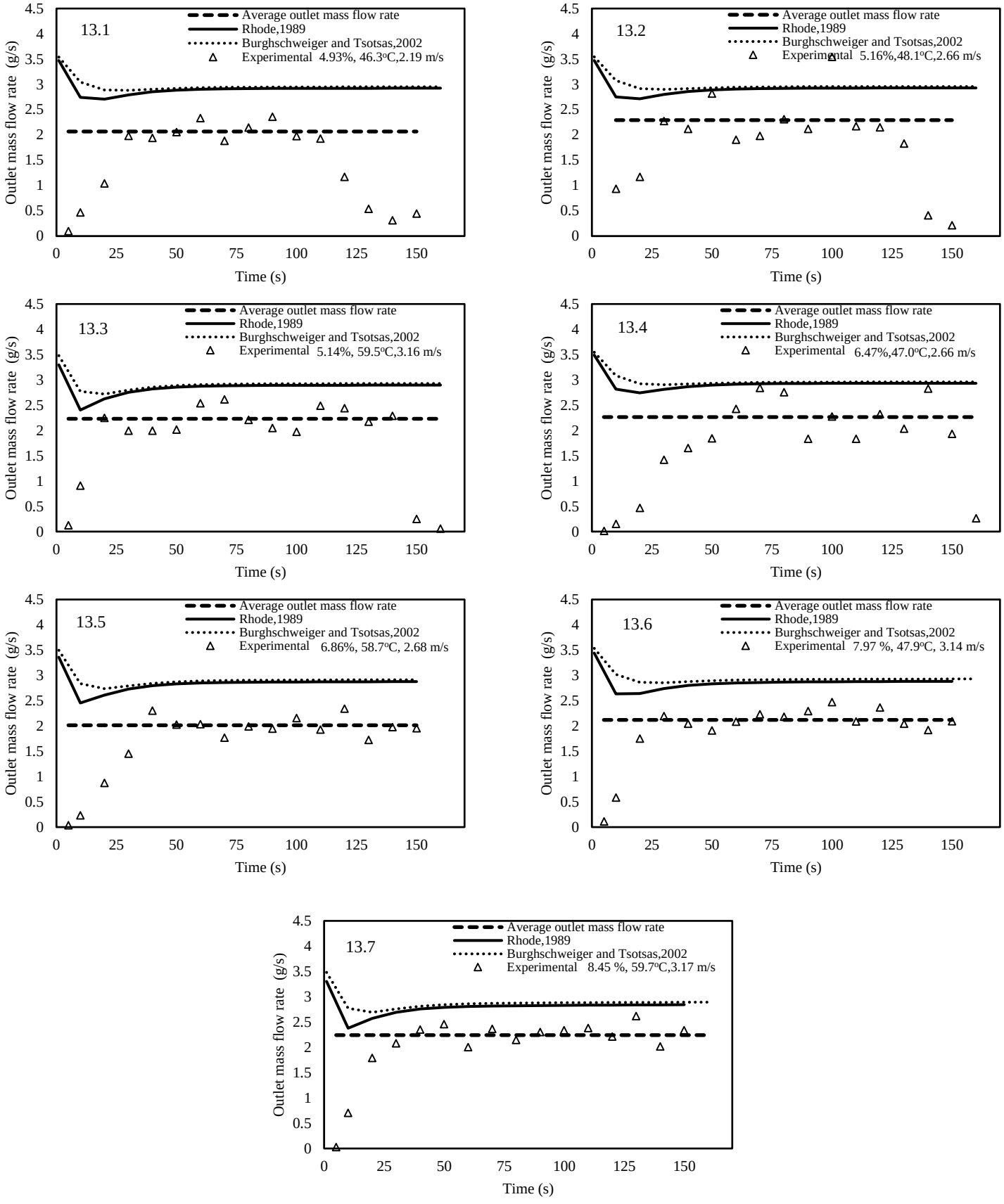

Figure A.2 . Outlet mass flow rate of the granules.

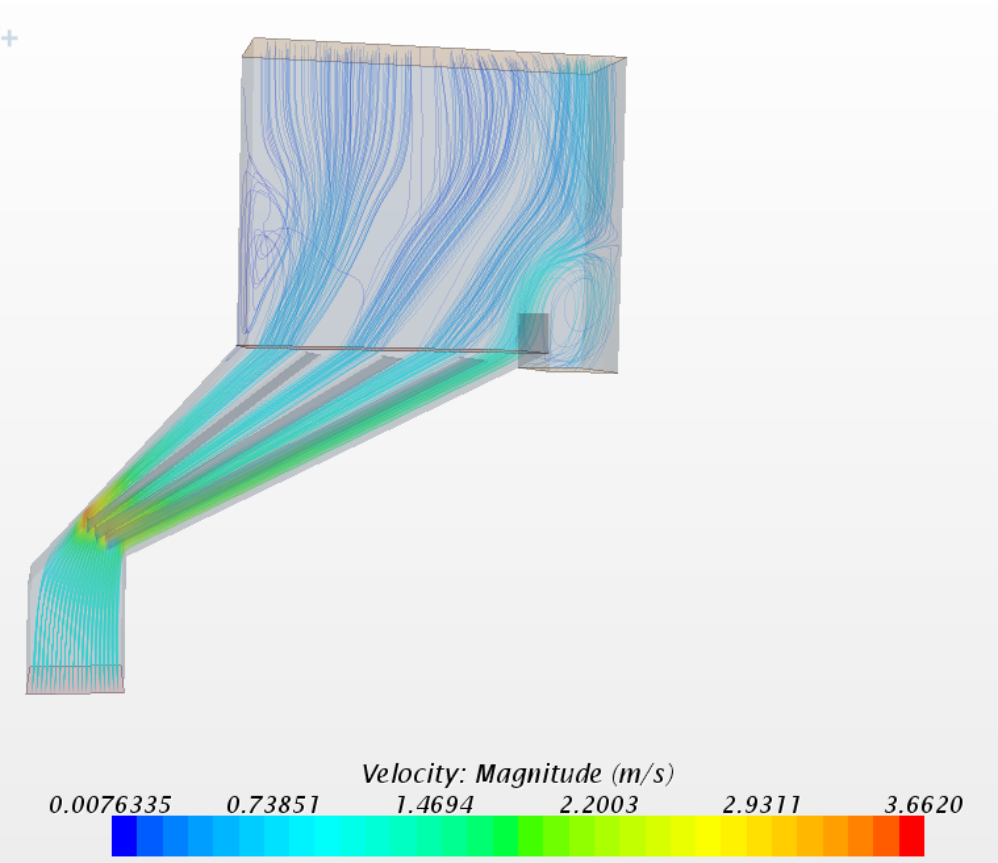

Figure A.3 Fluid pattern - CFD

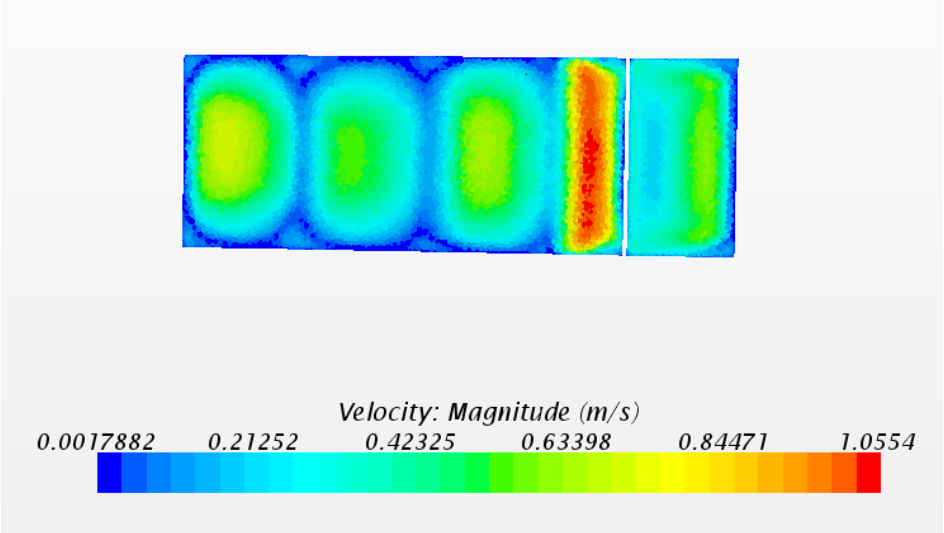

Figure A.4 Superficial velocity distribution over the free board

APPENDIX B: COMPUTATIONAL FLUID DYNAMICS & DISCRETE ELEMENTS METHODS PARAMETERS

Table B.1 Computational Fluid Dynamics Parameters

Air Viscosity (Pa-s)	$1.86\ 10^{-5}$
Particle diameter (μm)	1500
Particle density (kg/m^3)	1521.0

Table B.2 Parameters particle-particle for DEM

Hertz Mindlin	Static Friction Coefficient	0.5
	Normal Restitution Coefficient	0.5
	Tangential Restitution Coefficient	0.5
Linear Cohesion	Work of Cohesion	0.08 J/m^2
	Factor	1.5
Rolling Resistance		
Rolling Resistance Methods	Force Proportional	
Force Proportional	Coefficient of Rolling Resistance	0.005

Table B.3 Parameters particle-walls for DEM

Hertz Mindlin	Static Friction Coefficient	0.8
	Normal Restitution Coefficient	0.5
	Tangential Restitution Coefficient	0.5
Linear Cohesion	Work of Cohesion	0.08 J/m^2
	Factor	1.5
Rolling Resistance		
Rolling Resistance Methods	Force Proportional	
Force Proportional	Coefficient of Rolling Resistance	0.005

Table B.4 Turbulent model parameters

Realizable K-Epsilon Two-Layer	Buoyancy Production of Dissipation	Boundary Layer Orientation
	Cmu	0.09
	C1e	1.44
	C2e	1.9
	Ct	1.0
	Sigma_k	1.0
	Sigma_e	1.2
	Sarkar	2.0
	Tke Minimum	1.0E-10
	Tdr Minimum	1.0E-10
	Convection	2nd-order
	Two-Layer Type	Shear Driven (Wolfstein)
	Two-Layer ReY*	60.0
	Two-Layer Delta ReY	10.0